

# An Enhancement to an Electronic Stability Control System to Include a Rollover Control Function

Jianbo Lu, Dave Messih, Albert Salib and Dave Harmison

Ford Motor Company

Copyright © 2006 SAE International

## ABSTRACT

This paper proposes a method to enhance existing electronic stability control systems such that a certain level of rollover mitigation performance is achieved. Such an enhancement is conducted through a control algorithm using only the standard ESC sensors. The analysis presented here reveals that a rollover mitigation system such as this will face a trade-off between the vehicle's responsiveness and the control robustness due to error in the roll dynamics model and state estimation.

## 1. INTRODUCTION

Since its debut in 1995, electronic stability control (ESC) systems for automobiles have been implemented on various platforms [1]. Recently, the DOT announced a new proposal (Docket No. NHTSA-2006-25801, Proposed FMVSS 126) which would require all automotive manufacturers to begin equipping passenger vehicles under 10,000 pounds Gross Vehicle Weight with ESC systems starting with the 2009 model year and to have the feature available as standard equipment on all vehicles by the 2012 model year.

The traditional ESC systems aim to control the yaw and sideslip angle of a moving vehicle through individual wheel braking and engine torque reduction such that the desired path of a vehicle determined through the driver's inputs (e.g., steering input) can be maintained. That is, ESC systems typically help the vehicle to follow the driver's intent such that the driver maintains control of the vehicle regardless of the variation of the road conditions. Since they help to keep the vehicle on the road, ESC systems may reduce the occurrence of so-called tripped rollovers, which often occur when a vehicle departs from the road surface and account for approximately one third of all fatalities in single vehicle accidents.

In contrast to tripped rollover, the so-called un-tripped rollover occurs when a vehicle stays on the road. Such a rollover is also called a friction induced rollover due to the fact that it occurs when the tire lateral forces of the involved vehicle exceed certain thresholds for some duration during aggressive steering maneuvers. For a vehicle operated with loading that raises the center of gravity, an un-tripped rollover could occur when the

driver conducts an aggressive avoidance maneuver. In this paper, a function referred to as a Rollover Control Function (RCF), designed to mitigate un-tripped rollovers, is studied.

The simulation results studied in [2] and [3] indicate that an ESC system can increase a vehicle's resistance to un-tripped rollovers without enhancements specifically targeting rollover control. This may be because an oversteer condition is one of the important contributors to building up large tire lateral forces which can result in un-tripped rollovers. However, in some driving scenarios, oversteer control may not be sufficient to counteract an un-tripped rollover. If an un-tripped rollover can occur due to lateral force buildup when the vehicle is not oversteering (i.e. driver intent is maintained or the vehicle is understeering), additional control algorithms are needed to achieve rollover control. Additionally, the co-existence of traditional ESC functions and the RCF function will likely require a new function prioritization and arbitration.

The addition of a roll mitigation function in an ESC system has been actively pursued in recent years. For example, [4] describes an enhanced system over Driver Stability Control systems for commercial trucks. [5] proposes a stand-alone function called Anti-rollover Braking (ARB) when an impending rollover of a vehicle is sensed. In [6], engineers from Bosch describe a rollover mitigation function over its ESP system. Continental Teves has developed an Active Rollover Prevention (ARP) system. This paper provides some extension of the work developed in [7] which is similar in principle to [5], [6] and ARP but with a different control strategy. In addition to ESC-based brake control, other chassis control systems have also been pursued to mitigate rollovers, see [3], [9], [10], [11], [12] and [13] for more details.

This paper is organized as follows. A brief discussion about vehicle roll stability is provided section 2, with a discussion of a roll dynamics model based on standard ESC sensor information in section 3. Various wheel lift detection methods are briefly discussed in section 4. Finally, section 5 discusses the RCF control.

## 2. VEHICLE ROLL STABILITY

The vehicular roll instability studied here is the un-tripped rollover, where the vehicle has divergent roll motion along the vehicle's roll axis in response to steering inputs while driving on a smooth road.

Such an un-tripped rollover is typically induced by aggressive steering inputs. More specifically, it is the result of steering the vehicle so aggressively that the vehicle approaches its physical limit. Due to the divergence of the vehicle's roll motion, the vehicle can behave unpredictably. The roll stability studied in this paper is specifically dedicated to such an un-tripped rollover.

More rigorously, a vehicle is said to be roll stable if the roll angle between the vehicle body and the road surface is bounded by a threshold, called a rollover angle limit  $\gamma$ , when the vehicle is driven on a smooth road surface which may have an associated bank angle. Such a rollover angle limit  $\gamma$  is dependant on the vehicle loading condition, the driver's inputs and the road condition.

The above roll stability can also be characterized using the vertical travels of the wheel centers with respect to the smooth road surface. That is, a vehicle is said to be roll stable if it does not have sustainable two wheel lift from the road surface when the vehicle is driven on smooth roads.

A vehicle could experience an un-tripped rollover if it is not roll stable. Physically, the un-tripped rollover can be directly detected through sensors, for example, the laser height sensors which measure the distance of the vehicle body at the sensor mounting locations from the road surface along the direction of the laser beam.

Considering mounting 4 laser height sensors on the 4 corners of the vehicle body shown in Fig. 1, their outputs are denoted as  $z_{lf}, z_{rf}, z_{lr}$  and  $z_{rr}$  which measure the relative displacements of the vehicle corners at the left-front, right-front, left-rear and right-rear locations with respect to the road surface but defined on a body-fixed coordinate system  $b$  with axes  $b_1, b_2$  and  $b_3$  (called the body frame), more specifically, along the vertical direction  $b_3$  of the vehicle body. Let's define another coordinate system  $m$  with axes  $m_1, m_2$  and  $m_3$  which is attached to the road surface but moves and yaws with the vehicle body (called a moving road frame). Let  $t_s$  be the distance between the left and the right laser height sensors,  $b_s$  be the distance from the front to the rear laser height sensors. Let  $\theta_{x_{bm}}$  and  $\theta_{y_{bm}}$  be the relative roll and pitch angles between the vehicle body and the road surface which are approximately the Euler angles between the two coordinate systems  $b$  and  $m$ .

Define

$$\begin{aligned}\Theta_{x_{bm}} &= \frac{z_{lf} - z_{rf} + z_{lr} - z_{rr}}{2t_s} \\ \Theta_{y_{bm}} &= -\frac{z_{lf} + z_{rf} - z_{lr} - z_{rr}}{2b_s}\end{aligned}\quad (1)$$

then  $\theta_{x_{bm}}$  and  $\theta_{y_{bm}}$  now be expressed as:

$$\begin{aligned}\theta_{y_{bm}} &= \sin^{-1}\{\Theta_{y_{bm}}\} \\ \theta_{x_{bm}} &= \sin^{-1}\left\{\frac{\Theta_{x_{bm}}}{\cos(\theta_{y_{bm}})}\right\}\end{aligned}\quad (2)$$

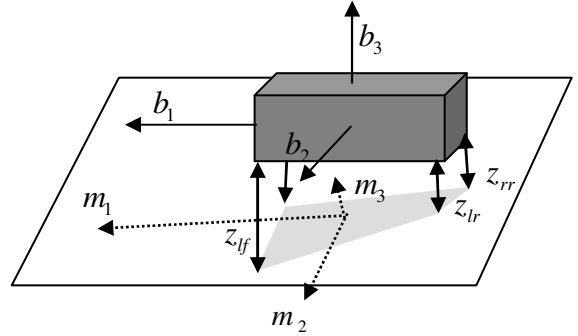


Fig.1. The body-fixed coordinated system, the moving road coordinate system and the height sensors.

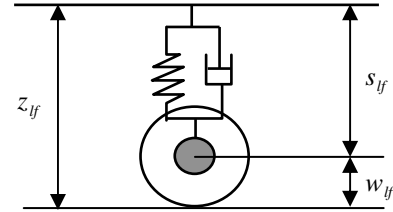


Fig. 2. The displacements of the wheel and the suspension system

The relative distance at the 4 corners can be further decomposed into the suspension stroke projected along the body vertical axis  $b_3$  and the wheel displacement between the road surface and the wheel centers which is also projected along  $b_3$  axis. Fig. 2 shows  $z_{lf}$  as an example. Notice that the suspension usually has different geometry and the suspension strokes are not necessarily parallel to the vehicle body axis. If the four suspension strokes are denoted as  $s_{lf}, s_{rf}, s_{lr}$  and  $s_{rr}$ , the four wheel center displacements are denoted as  $w_{lf}, w_{rf}, w_{lr}$  and  $w_{rr}$ , then we have

$$\begin{aligned}z_{lf} &= \Pi_f s_{lf} + \pi_f w_{lf} \\ z_{rf} &= \Pi_f s_{rf} + \pi_f w_{rf} \\ z_{lr} &= \Pi_r s_{lr} + \pi_r w_{lr} \\ z_{rr} &= \Pi_r s_{rr} + \pi_r w_{rr}\end{aligned}\quad (3)$$

where  $\Pi_f$  and  $\Pi_r$  are the projection operators that project the front and rear suspension strokes to the body vertical axis  $b_3$ , and  $\pi_f$  and  $\pi_r$  are the ratios to convert the tire displacement from the wheel location to the laser height sensor location.

The suspension contributions in  $\theta_{x_{bm}}$  and  $\theta_{y_{bm}}$ , which are called suspension roll and pitch angles, can be expressed as in the following

$$\begin{aligned}\Theta_{x_{bw}} &= \frac{\Pi_f s_{lf} - \Pi_f s_{rf} + \Pi_r s_{lr} - \Pi_r s_{rr}}{2t_s} \\ \Theta_{y_{bw}} &= \frac{\Pi_r s_{lr} - \Pi_f s_{lf} + \Pi_r s_{rr} - \Pi_f s_{rf}}{2b_s}\end{aligned}\quad (4)$$

And similarly, the wheel contributions in  $\theta_{x_{bm}}$  and  $\theta_{y_{bm}}$ , which are called the wheel departure roll and pitch angles, can be expressed as

$$\begin{aligned}\Theta_{x_{wm}} &= \frac{\pi_f w_{lf} - \pi_f w_{rf} + \pi_r w_{lr} - \pi_r w_{rr}}{2t_s} \\ \Theta_{y_{wm}} &= \frac{\pi_r w_{lr} - \pi_f w_{lf} + \pi_r w_{rr} - \pi_f w_{rf}}{2b_s}\end{aligned}\quad (5)$$

Then

$$\Theta_{x_{bm}} = \Theta_{x_{bw}} + \Theta_{x_{wm}}, \Theta_{y_{bm}} = \Theta_{y_{bw}} + \Theta_{y_{wm}} \quad (6)$$

Notice that although the relationship in (2) is nonlinear, the decomposition in (6) is linear if we work with  $\Theta_{x_{bm}}$  and  $\Theta_{y_{bm}}$  in place of  $\theta_{x_{bm}}$  and  $\theta_{y_{bm}}$ . Also considering that for the controlled vehicle discussed here, the magnitude of  $\theta_{x_{bm}}$  and  $\theta_{y_{bm}}$  are small (e.g. less than 10 degrees),  $\Theta_{x_{bm}}, \Theta_{y_{bm}}, \Theta_{x_{bw}}, \Theta_{y_{bw}}, \Theta_{x_{wm}}$  and  $\Theta_{y_{wm}}$  will be very close to the true angles of  $\theta_{x_{bm}}, \theta_{y_{bm}}, \theta_{x_{bw}}, \theta_{y_{bw}}, \theta_{x_{wm}}$  and  $\theta_{y_{wm}}$ . For this reason, in the sequential discussion,  $\Theta_{x_{bm}}, \Theta_{y_{bm}}, \Theta_{x_{bw}}, \Theta_{y_{bw}}, \Theta_{x_{wm}}$  and  $\Theta_{y_{wm}}$  will be interchangeably used with  $\theta_{x_{bm}}, \theta_{y_{bm}}, \theta_{x_{bw}}, \theta_{y_{bw}}, \theta_{x_{wm}}$  and  $\theta_{y_{wm}}$ .

Defining the time duration after a time instant  $t$  such that the magnitude of the body-to-road roll angle  $\Theta_{x_{bm}}$  is beyond a threshold  $\gamma$  as the following

$$\tau(t, \gamma) = \max\{\Delta t : |\Theta_{x_{bm}}(\tau)| \geq \gamma \text{ for } t < \tau \leq t + \Delta t\} \quad (7)$$

Then the vehicle is roll stable if  $\tau(t, \gamma)$  is below a threshold  $\varepsilon_\gamma$ . Notice that although the above definition of the roll stability is rather kinematics in nature, the threshold used is dynamics dependant.

Although the aforementioned laser height sensors were instrumented in the target vehicle, their implementation in mass production to detect the vehicle rollover condition is generally cost prohibitive with the current technology. In practice, we are pursuing using the standard ESC sensors to detect roll instability. While [8], [9] and [14] use an extra roll rate sensor together with the information from ESC systems to detect the roll instability, this paper focuses on rollover detection without using a roll rate sensor. In the following section, such a roll dynamics sensing method and its limitation in achieving robust detection are discussed.

### 3. ROLL DYNAMICS MODELING

In order to use the available sensors in ESC to detect vehicular roll instability, the vehicle roll dynamics need to be related to the sensor signals. The standard ESC sensors include a yaw rate, a lateral accelerometer, a steering wheel angle sensor, four wheel speed sensors, a master cylinder pressure sensor and oftentimes a longitudinal accelerometer. Additionally, some of the calculated variables in ESC such as the vehicle reference velocity, the estimated brake caliper pressures, and the individual wheel control status will also be used.

The motion sensors of longitudinal acceleration (optional in ESC), lateral acceleration and yaw rate are packed in a sensor cluster which is rigidly mounted on the body close to the vehicle's center of gravity. Denote the offset compensated and filtered longitudinal acceleration as  $a_{xs}$ , lateral acceleration as  $a_{ys}$  and yaw rate as  $\omega_{zs}$ . Denote the coordinate system defining the sensor signals as frame  $s$  (called a sensor frame). Generally speaking the sensor frame  $s$  and the body frame  $b$  do not coincide due to sensor cluster mounting error and sensor element alignment error within the cluster. Denote the vehicle reference velocity calculated in ESC as  $v_{xref}$ . If we align the laser height sensors with vertical direction of the sensor frame  $s$ , the similar angles to those defined in the last section can be also defined as  $\Theta_{x_{sm}}$  and  $\Theta_{y_{sm}}$ ,  $\Theta_{x_{sw}}$ ,  $\Theta_{y_{sw}}$ .

Notice that an accelerometer measures the total acceleration along the sensor measurement direction, including the influence of gravity. The lateral acceleration of the vehicle body at its c.g. location projected on the lateral axis of the  $s$  frame can be expressed as

$$a_{ycgs} = a_{ys} + l_{s2cg} \dot{\omega}_{zs} \quad (8)$$

where  $l_{s2cg}$  is the distance between the origin of the ESC motion sensor cluster and the c.g. of vehicle body.

In order to relate the vehicle roll dynamics with the sensor signals defined in the sensor frame, the vehicle's suspension kinematics and compliance information is

needed. In this paper, we consider an SUV with a front independent suspension and a rear solid suspension. Due to the constraints of the rigid links in the suspension, the vehicle body can only roll and pitch along a fixed direction, which is called the roll and pitch axes. Notice that the roll and pitch axes are usually different from the vehicle's body-fixed longitudinal and lateral axes. From Fig. 3 for the SUV of interest, the front roll center is close to the ground, and the rear roll center is close to the vehicle floor.

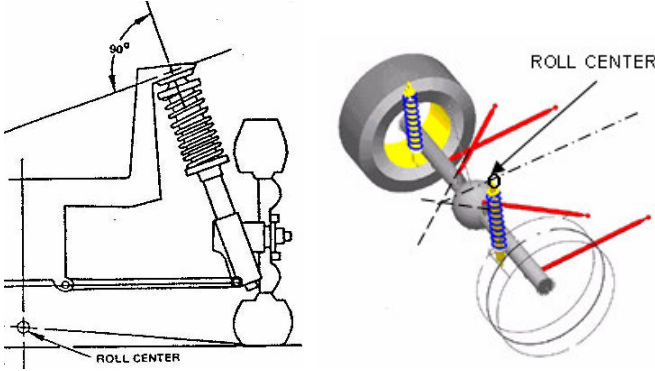


Fig. 3. Left: front independent suspension. Right: rear solid suspension.

### 3.1. Roll Sensing Based on Vehicle Body Model

Let  $F_{yf}$  and  $F_{yr}$  be the resultant forces along the lateral direction of the motion sensor but applied to the vehicle body through the front and rear roll centers. Let the vertical distance from the vehicle body c.g. location to the front and rear roll centers be  $h_f$  and  $h_r$ . Using Newton's law in the sensor frame  $s$ , we obtain the following equations of motion

$$\begin{aligned} M_s a_{ycgs} &= F_{yf} + F_{yr} \\ I_z \dot{\omega}_{zs} &= F_{yf} b_f - F_{yr} b_r \\ I_x \dot{\omega}_{xs} &= F_{yf} h_f + F_{yr} h_r - M_{roll} \end{aligned} \quad (9)$$

where  $I_x$  and  $I_y$  are the moment of inertia of the car body with respect its body axes;  $M_s$  is the sprung mass (the mass of the car body);  $b_f$  and  $b_r$  are the distance of the vehicle body c.g. to the front and rear axles with  $b = b_f + b_r$ .

The roll moment due to the suspension forces is computed as

$$\begin{aligned} M_{roll} &= l \Pi_f (K_f s_{lf} + D_f \dot{s}_{lf} - K_f s_{rf} - D_f \dot{s}_{rf}) \\ &+ l \Pi_r (K_r s_{lr} + D_r \dot{s}_{lr} - K_r s_{rr} - D_r \dot{s}_{rr}) \\ &+ K_{arf} l^{-1} \Pi_f (s_{lf} - s_{rf}) + K_{arr} l^{-1} \Pi_r (s_{lr} - s_{rr}) \\ &= K_{roll} \Theta_{xsw} + D_{roll} \dot{\Theta}_{xsw} \end{aligned} \quad (10)$$

where  $l$  is the distance between the left and right suspensions;  $K_f$  and  $K_r$  are the front and rear suspension spring rates;  $K_{arf}$  and  $K_{arr}$  are the stiffness of the front and the rear anti-roll bars.  $D_f$  and  $D_r$  are the front and the rear suspension damping rates.  $K_{roll}$  and  $D_{roll}$  are the equivalent roll stiffness and roll damping rate for the suspension.

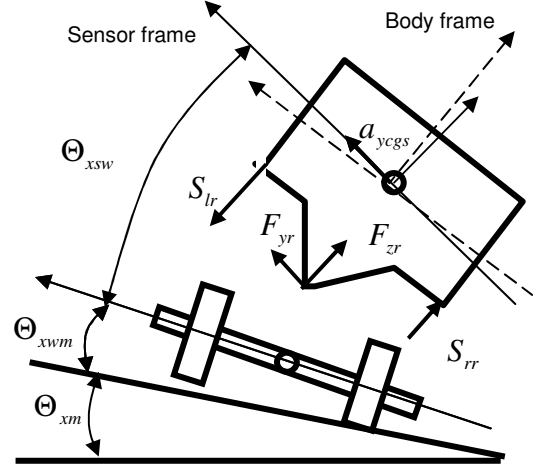


Fig.4. A vehicle during a rollover event on a banked road.

From (9), the lateral tire forces defined on the sensor frame but applied to the vehicle body through its front and rear roll centers can be computed as in the following

$$\begin{aligned} F_{yf} &= (M_s a_{ycgs} b_r + I_z \dot{\omega}_{zs}) / b \\ F_{yr} &= (M_s a_{ycgs} b_f - I_z \dot{\omega}_{zs}) / b \end{aligned} \quad (11)$$

and the vehicle body roll acceleration defined in the sensor frame can be estimated as in the following

$$\dot{\omega}_{xs} = c_0 \dot{\omega}_{zs} - c_1 \Theta_{xbw} - c_2 \dot{\Theta}_{xbw} + c_3 a_{ycgs} \quad (12)$$

where the coefficients  $c_1, c_2, c_3, c_4$  are defined as

$$\begin{aligned} c_0 &= (h_f - h_r) I_z / I_x / b \\ c_1 &= K_{roll} / I_x \\ c_2 &= D_{roll} / I_x \\ c_3 &= (h_f b_r + h_r b_f) M_s / I_x / b \end{aligned}$$

A similar discussion could lead to the following for pitch acceleration estimation

$$\dot{\omega}_{ys} = d_0 \Theta_{ybw} + d_1 \dot{\Theta}_{ybw} + d_2 a_{xs} \quad (13)$$

where the coefficients  $d_0, d_1$  and  $d_2$  can be similarly obtained.

Considering the roll rate in (12) can be related to the other roll angles as in the following

$$\omega_{xs} = \dot{\Theta}_{xsm} + \dot{\Theta}_{xm} + \omega_{zs}\Theta_{ys} \quad (14)$$

where  $\Theta_{xsm}$  is the relative roll angle between the sensor frame and the moving road surface, i.e., it is the sum of the suspension roll angle  $\Theta_{xbw}$  and the wheel departure angle  $\Theta_{xwm}$ .  $\Theta_{ys}$  is the pitch angle between the sensor frame and the horizon, which can be approximated using the sensor signals as

$$\Theta_{ys} \approx \frac{a_{xs} - \dot{v}_{xref}}{g}$$

$\Theta_{xm}$  is the angle between the horizon and the road surface, or the road bank angle, as shown in Fig. 4. Based on (12) and (14) and taking the Laplace transform, we obtain the relative roll angle between the sensor frame and the moving road frame:

$$\Theta_{xsm} = T_1(s)a_{yscg} + T_2(s)(c_0\omega_{zs} - [\omega_{zs}\Theta_{ys}]) - T_3(s)(\Theta_{xm} + \Theta_{xwm}) + \Theta_{xwm} \quad (15)$$

where the transfer functions are defined as

$$\begin{aligned} T_1(s) &= \frac{c_3}{s^2 + c_2s + c_1} \\ T_2(s) &= \frac{s}{s^2 + c_2s + c_1} \\ T_3(s) &= \frac{s^2}{s^2 + c_2s + c_1} \end{aligned} \quad (16)$$

Equation (15) shows that  $\Theta_{xsm}$ , which reflects the relative roll angle between the vehicle body and the road, is a function of the road bank angle, the wheel departure roll angle, the vehicle lateral acceleration and the vehicle yaw rate.

Since  $T_3(s)$  in (15) is the form of a high-pass filter, when the wheel departure roll angle is very dynamic (consisting of high frequency content), then (15) can be further simplified as

$$\Theta_{xsm} = T_1(s)a_{yscg} + T_2(s)(c_0\omega_{zs} - [\omega_{zs}\Theta_{ys}]) - T_3(s)\Theta_{xm}$$

which indicates that the roll angle from the sensor frame to the moving road frame is influenced by the road bank.

If the sum  $\Theta_{xm} + \Theta_{xwm}$  has only low frequency content (i.e., the wheel lifts slowly from the horizon), then (15) can be simplified as

$$\Theta_{xsm} = T_1(s)a_{yscg} + T_2(s)(c_0\omega_{zs} - [\omega_{zs}\Theta_{ys}]) + \Theta_{xwm}$$

which implies that the roll angle between the sensor frame and the moving road frame is influenced by the wheel departure roll angle.

### 3.2. Roll Sensing Based on a Rear Wheel Model

The aforementioned roll model of the vehicle body demonstrates the necessity of characterizing wheel departure roll angle in determining the relative roll angle between the sensor frame and the road. Now let's compute such a wheel departure roll angle based on the wheel roll model.

The vehicle of interest has rear wheel lift earlier than front wheel lift due to the tilted roll axis. Hence the roll dynamics of the rear solid axle are a good early indication of a potential vehicle rollover. Based on the force balancing on the rear wheel set shown in Fig. 5 with the assumption that the vertical motion of the c.g. of the wheel set is only due to its roll motion, the roll dynamics after wheel lift has occurred are

$$\begin{aligned} I_{xwr}\dot{\omega}_{xwr} &= F_{yr}H_r \cos \Theta_{xsw} - F_{zr}H_r \sin \Theta_{xsw} + \\ &F_{yrm}(r_0 \cos \Theta_{xwm} + t_r \sin \Theta_{xwm}) - \\ &F_{zrm}t_r \cos \Theta_{xwm} + M_{rollr} \\ M_{wr}[a_{yrs} + \dot{\omega}_{xs}(H_r + h_r \cos \Theta_{xsw})] &= F_{yr} + \\ &F_{yrm} \cos \Theta_{xsm} + F_{zrm} \sin \Theta_{xsm} \\ M_{wr}[t_r\dot{\omega}_{xwr} + g \cos(\Theta_{xwm} + \Theta_{xm})] &= F_{zrm} - \\ &F_{zr} \cos \Theta_{xsw} - F_{yr} \sin \Theta_{xsw} \end{aligned} \quad (17)$$

where  $\omega_{xwr}$  denotes the roll rate of the rear wheel set,  $I_{xwr}$  its roll moment of inertia,  $M_{wr}$  its mass,  $r_0$  the rolling radius of the tire,  $t_r$  the half track of the wheel,  $H_r$  is the distance from the rear roll center to the center of the rear axle,  $M_{rollr}$  the roll moment applied from the rear suspension to the wheel set which can be approximated as  $M_{rollr} = M_{roll}b_r/b$ ,  $F_{yrm}$  the lateral force applied to the outside wheel from the moving road frame,  $F_{zrm}$  the normal force applied to the outside wheel.  $F_{zr}$  is the vertical force applied to the wheel set through the rear roll center, and can be estimated from longitudinal acceleration and the vehicle's static mass distribution.

Based on equations in (17), the wheel set roll acceleration  $\dot{\omega}_{xwr}$  can be expressed as a linear function of  $F_{yr}$ ,  $F_{zr}$ ,  $M_{roll}$ ,  $a_{ys}$  and  $\omega_{xs}$  but with nonlinear dependence on various angles such as  $\Theta_{xsw}$ , the wheel departure roll angle  $\Theta_{xwm}$  and the road bank angle  $\Theta_{xm}$ .

Notice that the wheel departure roll angle satisfies the following relationship

$$\dot{\Theta}_{xwm} \approx \omega_{xwr} - \dot{\Theta}_{xm} \quad (18)$$

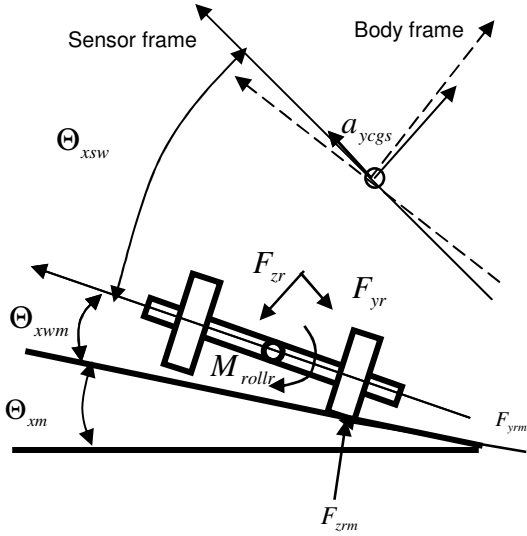


Fig.5. The forces applied to the rear wheel set.

Using the small angle approximation, (17) can be reduced to

$$\begin{aligned} I_{xwr}\dot{\omega}_{xwr} &\approx F_{yr}H_r - F_{zr}H_r\Theta_{xsw} + \\ &F_{yrm}(r_0 + t_r\Theta_{xwm}) - \\ &F_{zrm}t_r + M_{rollr} \\ M_{wr}[a_{yrs} + \dot{\omega}_{xs}(H_r + h_r)] &\approx F_{yr} + F_{yrm} + \\ &F_{zrm}\Theta_{xsm} \\ M_{wr}[t_r\dot{\omega}_{xwr} + g] &\approx F_{zrm} - F_{zr} - F_{yr}\Theta_{xsw} \end{aligned} \quad (19)$$

Combining (18) and (19), the 4 unknowns can be solved from the 4 equations. The 4 unknowns are  $\Theta_{xwm}$ ,  $\omega_{xwr}$ ,  $F_{yrm}$  and  $F_{zrm}$ . By eliminating the other three unknowns, a second order differential equation for  $\Theta_{xwm}$  can be generated. Therefore, the wheel departure angle is a function of  $\Theta_{xsw}$ , lateral acceleration  $a_{ycgs}$ , and yaw rate  $\omega_{zs}$  and road bank angle  $\Theta_{xm}$ .

Notice that the aforementioned computation will need to know when the computation should begin, i.e., when wheel lift initiates. Due to sensor offsets and low frequency drifts, a wash-out filter is used to compute the wheel departure roll angle  $\Theta_{xwm}$  in the above computation. Since  $\Theta_{xsw}$  satisfies

$$\dot{\Theta}_{xsw} \approx \omega_{xs} - \omega_{xwr}$$

the only variable which is not available for the aforementioned model is the road bank,  $\Theta_{xm}$ . Certain assumptions about  $\Theta_{xm}$  can be made, for example, during a rollover event, the road bank may be assumed

to stay as constant. Another way to condition road bank angle in the above computation is taking into account the other variables. For example, during a wheel lift event,  $\Theta_{xsw}$  is saturated at a certain level due to suspension travel limitations, and its rate of change is close to zero.

### 3.3. Implementation Oriented Roll Approximation

Based on the discussion above, one can conclude that the key variable used in control, namely, the relative roll angle between the vehicle body and the road surface is influenced by the road bank angle, the wheel departure angle, the vehicle's cornering acceleration, the vehicle's c.g., etc.

Roof loading can significantly change the roll moment of inertia  $I_x$  and the sprung mass  $M_s$  used in (9), hence the computation of  $\Theta_{xsm}$  in (15) using the aforementioned model-based approach through sensor signals is also influenced by roof loading.

If in (15), the road bank angle changes slowly, while the wheel departure roll angle varies quickly, we could obtain the approximation  $\Theta_{xsm} \approx \hat{\Theta}_{xsm}$ , where

$$\hat{\Theta}_{xsm} = T_1(s)a_{ycgs} + T_2(s)(c_0\omega_{zs} - [\omega_{zs}\Theta_{ys}]) \quad (20)$$

(20) is a good approximation of  $\Theta_{xsm}$  if the vehicle is driven on a smooth flat road surface without wheels lifted from the road. Notice that, if  $\hat{\Theta}_{xsm}$  is tuned for a vehicle without roof loading, its magnitude will be significantly smaller than that of the true  $\Theta_{xsm}$  of the vehicle with roof loading, and if it is tuned for vehicle with roof loading, its magnitude will be significantly larger than that of the true  $\Theta_{xsm}$  of the vehicle without roof loading.

Additionally, if the vehicle is experiencing slow wheel lift or dynamic road bank variation,  $\hat{\Theta}_{xsm}$  computed in (20) will be significantly different from the true  $\Theta_{xsm}$ .

In order to implement a rollover control, we compute a roll-signal-for-control  $\Theta_{x-ctr}$  based on a weighted computation of  $\hat{\Theta}_{xsm}$  and  $\hat{\Theta}_{xwm}$  (see section 3.2)

$$\Theta_{x-ctr} = W_1\hat{\Theta}_{xsm} + W_2\hat{\Theta}_{xwm} \quad (21)$$

where  $W_1$  is a weight that is a function of the wheel lift status and the other sensor or computed signals, and  $W_2$  is another weight based on the confidence of the computation of the wheel departure roll angle  $\hat{\Theta}_{xwm}$ .

Figure 6 and Figure 7 display computations based on sensor data in a vehicle tested on level ground. Figure 6 shows  $\hat{\Theta}_{xsm}$  tuned for maximum-allowed loading, where the vehicle is equipped with outriggers and roof loading (with ESC off). It shows that during a wheel lift event,

$\hat{\Theta}_{xsm}$  is saturated around -5.5 degrees, while the true roll angle  $\Theta_{xsm}$  exceeds -16 degrees.

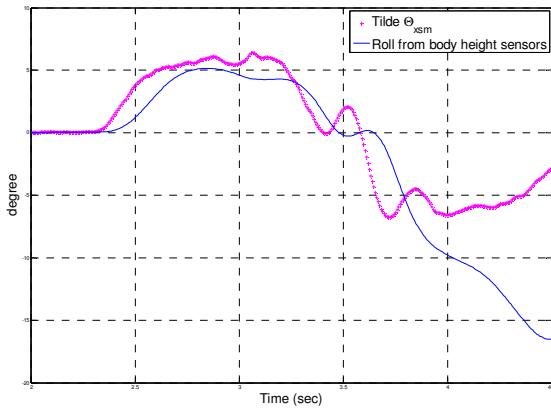


Fig. 6. Comparison between  $\hat{\Theta}_{xsm}$  and the true roll angle based on body height sensors during a two wheel lift event for a vehicle with a roof loading

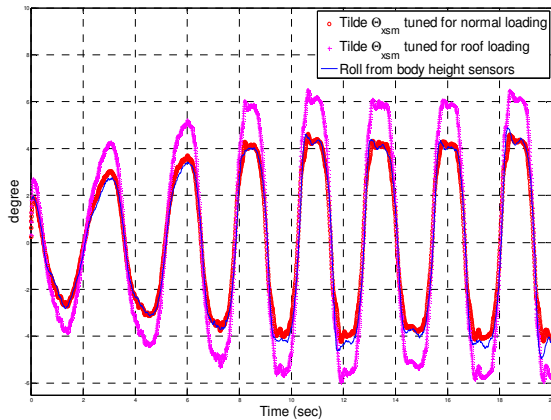


Fig. 7. The comparison between  $\Theta_{x-ctr}$  and the true roll angle based on body height sensors during a slalom maneuver on a level ground.

Fig. 7 shows the computation of  $\hat{\Theta}_{xsm}$  in a slalom on level ground for a vehicle equipped with and without roof load. If  $\hat{\Theta}_{xsm}$  is tuned for a vehicle with roof loading, to characterize the roll angle between vehicle body and the road surface, it overestimates for a vehicle without roof loading. On the other hand, if  $\hat{\Theta}_{xsm}$  is tuned for a vehicle without roof loading, it significantly underestimates for vehicles with roof loading.

One can conclude that the ESC sensor set alone can not provide all the necessary information to calculate a relative roll angle between the vehicle body and the road surface that is robust to varying load conditions and varying road bank.

Since  $\hat{\Theta}_{xsm}$  is used as a feedback control variable, the underestimation of the true roll angle leads to potential

ineffectiveness of the brake control. On the other hand, overestimation of the true signal leads to unnecessary brake control activations. Therefore, using lateral acceleration as the key input to characterizing the vehicle roll dynamics will result in making a trade-off in the control.

## 4. WHEEL LIFT DETECTION

In order to determine when the vehicle is experiencing wheel lift such that the wheel departure roll angle can be computed based on model (15), or to prepare the brake hydraulics for large brake pressure buildup, various wheel lift detections are conducted together with vehicle roll determination. Three aspects of wheel lift detection are studied here: (i) Active Wheel Lift Detection (AWLD), (ii) Passive Wheel Lift Detection (PWLD) and (iii) Integration of AWLD and PWLD.

### 4.1. Active Wheel Lift Detection

AWLD is used to determine if a wheel is lifted or grounded by checking the wheel rotation in response to a given brake pressure. It utilizes signals from the brake control system such as the wheel speed sensor signals, the individual estimation of each of the brake caliper pressures, etc. More specifically, it sends a small brake pressure to an inside wheel, then checks the response of that lightly braked wheel. If the vehicle lateral acceleration sensor indicates a hard cornering of the vehicle on a high mu surface and the inside wheel experiences a longitudinal slip ratio larger than a threshold in response to a relatively small brake pressure, then this inside wheel is likely to be lifted from the ground. In order to differentiate the slip ratio of the inside wheel generated from the low mu surface from the one of the inside wheel generated from the lifted wheel during high mu maneuvers, AWLD is activated when the vehicle achieves a certain level of cornering acceleration.

Implementing AWLD requires special considerations to address system interactions. Notice that during driver braking, a lightly braked but lifted wheel will likely initiate ABS to dump the brake pressure. The initial pressure build caused by the driver braking, followed by the ABS action is similar to AWLD. On the other hand, in order to maximize brake pressure build rate on the control wheel, AWLD brake pressure is inhibited for the wheel that is on the same hydraulic circuit as the control wheel.

Due to the reactive nature of this strategy, a lifted wheel detected by AWLD suffers a time delay which can be several hundred milliseconds. Namely, if the control brake pressure command is solely based on a PL or AL status in AWLD algorithm, the hydraulics can not provide sufficient pressure to control the vehicle instability. A significant advantage of AWLD is the ability to reduce potentially unnecessary activations when a PG or AG is detected.

## 4.2. Passive Wheel Lift Detection

The intent of PWLD is to determine if a wheel is lifted or grounded by checking the vehicle dynamics and wheel speed behavior without actively requesting brake pressures. Namely, it passively monitors the wheel speeds to determine if the speeds indicate a potential wheel lift condition.

One aspect of PWLD can be characterized by rolling radius-based axis roll angle, which captures the angle between the wheel axle and the average road surface through the dynamic rolling radii of the left and right wheels. Since the computation of the rolling radius is related to the wheel speed and the linear velocity of the vehicle at each of the four corners, such a rolling-radius based wheel departure angle will assume abnormal values when there are large wheel slips. This happens when a wheel is lifted and there is torque applied to the wheel. Therefore, if this rolling radius-based wheel departure angle is increasing rapidly during a maneuver with large cornering acceleration, the vehicle may have lifted wheels. A small magnitude of this angle indicates the wheels are likely grounded.

PWLD can also be conducted by considering the normal loading sustained at each wheel. Theoretically, when a wheel's normal loading decreases to zero, this indicates that the wheel is no longer contacting the road surface. A large magnitude of this loading indicates that the wheel is likely grounded.

Another aspect of PWLD compares the actual road torques applied to the wheels and the road torques which are needed to sustain the wheels when they are grounded. The actual road torques can be obtained through torque balancing for each wheel using wheel acceleration, estimated engine torque and estimated brake torque. If the wheel is contacting the road surface, the calculated actual road torques must match or be larger than the torques determined from the nonlinear torques calculated from the normal loading and the longitudinal slip at each wheel.

Finally, PWLD can be conducted by checking wheel longitudinal slip. If during a normal braking or throttle apply, the wheels on the inner curve side of the vehicle experience increased magnitude of slip, then those wheels are losing longitudinal road torque, which implies that the wheels could be lifted during maneuvers involving large cornering acceleration.

Notice that all the methods in PWLD are conducted when the vehicle achieves substantial cornering acceleration (e.g., greater than 0.5 g).

## 4.3. Integration of AWLD and PWLD

In order to capitalize on the benefits of AWLD during steady-state driving conditions and the instantaneous nature of PWLD, an integration of AWLD and PWLD is required.

The wheel lift status for each wheel is set to one of 5 levels. The 5 levels are: absolutely grounded (AG), possibly grounded (PG), no indication (NI), possibly lifted (PL) and absolutely lifted (AL).

Fig. 8 illustrates the integration of AWLD and PWLD. A detailed description of the above wheel lift detection methods can be found in [15].

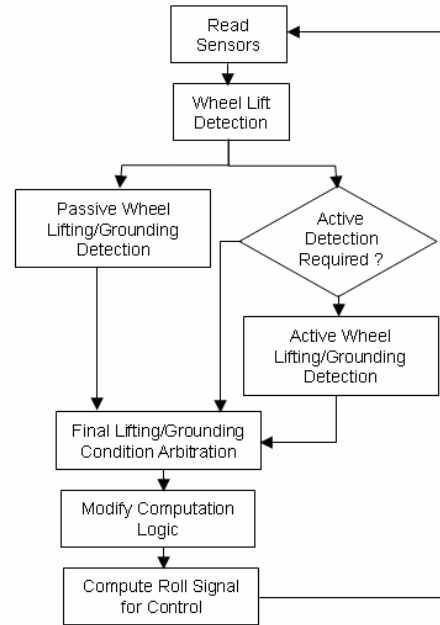


Fig. 8. The integration between AWLD and PWLD

## 5. ROLLOVER CONTROL FUNCTION

In this section, the RCF control structure will be discussed. Fig. 9 provides a schematic overview of RCF.

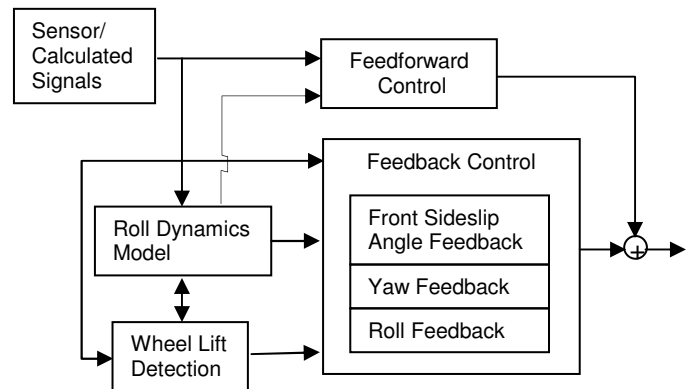


Fig. 9. RCF Algorithm Integration



## 5.1. Mechanism to Reduce Roll Moment

The front tire lateral force projected on the plane perpendicular to the roll axis is the main reaction force causing un-tripped rollovers. Such a force is called the effective lateral tire force (ELTF). (11) provides a simple characterization of ELTF. Notice that a rollover is unlikely to happen for maneuvers with a higher frequency of steering input such as an aggressive slalom, where the ELTF does not have a long duration in any single vehicle cornering direction. However, a rollover is more likely for maneuvers with steering input of medium frequency, where the ELTF has a longer duration to accumulate and can be sustained at critical levels. A similar situation could occur during a maneuver with a mixed high and low frequency steering input such as a fishhook or a J-turn. Due to the tire friction circle, braking can be used to effectively reduce the buildup of the ELTF.

## 5.2. Control Signals

In order to execute RCF, a large brake pressure is requested on the front outside wheel during potentially unstable events. When RCF requests the maximum pressure build rate, significant delays in brake pressure buildup can occur. Therefore, if a brake pressure buildup is requested after the roll instability is underway there may not be sufficient time to build an adequate control pressure to mitigate the event. The control effectiveness would be even less robust if the vehicle has large roof load. To deal with such a brake pressure build delay, a feedforward control is used to pre-charge the hydraulic system. Such a feedforward control utilizes the prediction information based on the driver's steering and the other vehicle state information to provide a pressure build prior to the roll instability. Note that this pre-charge is designed to minimize pressure build delay, and therefore is a relatively small pressure to establish a speed in the brake controls pump and reduce caliper knockback.

The feedback control used in RCF is a coordination and combination of three feedback control commands based on three different control signals.

One of the feedback control signals used in RCF is  $\Theta_{x-ctr}$  computed in (21). The feedback brake pressure command from  $\Theta_{x-ctr}$  uses a PD feedback control where the control gains and deadbands are functions of various sensor and computed signals. As we discussed before,  $\Theta_{x-ctr}$  is not able to adapt to various vehicle loading conditions, resulting in an unavoidable trade-off. For example, if the PD control gains and deadbands are tuned for a vehicle with roof loading, although the control might be effective for vehicles with roof loading, it will cause unnecessary brake activation during dynamic maneuvers for vehicles without roof loading. Such unnecessary braking might inhibit the responsiveness of the vehicle. Conversely, if the PD gains and deadbands are tuned for a vehicle without roof loading, it will not be optimized to mitigate rollover in a vehicle with roof loading.

Since the road bank angle influences the computation of  $\Theta_{x-ctr}$  which is mainly influenced by the vehicle lateral acceleration, the PD control based on  $\Theta_{x-ctr}$  will need to conduct a similar trade-off between a banked road and level ground.

Due to limited hydraulic capabilities, a leading indicator of  $\Theta_{x-ctr}$  is needed to sufficiently control potential rollover events. Therefore another control signal used in RCF is the model-based linear sideslip angle,  $\beta_{flin}$ , at the front axle, which is the front tire lateral force times the front tire compliance.

The control based on  $\beta_{flin}$  significantly leads the  $\Theta_{x-ctr}$  control. However,  $\beta_{flin}$  also has the potential to be relatively erratic, potentially leading to a premature reduction in control. Therefore, a robust signal is needed to fill in the resulting control gap between  $\beta_{flin}$  and  $\Theta_{x-ctr}$  control. A yaw rate-based PD controller can accomplish this, and is implemented as shown in Fig. 10.

In such a control structure including three feedback controllers and a feedforward controller, the phasing in a fishhook maneuver would be such that a particular controller is dominant as the transitional maneuver progresses (see Fig. 10).

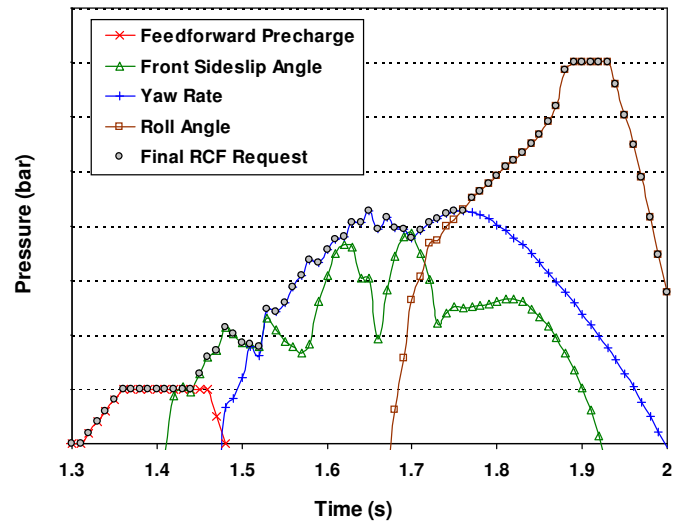


Fig. 10. Pressure Profile of RCF Control Event

## 5.3. Arbitration and Integration

The ESC system gives a driver full ability to control the vehicle, but with intervention when needed to help the vehicle follow the driver's intent. One of the biggest differentiators between ESC and the rollover control function is that the brake control is no longer solely in response to driver intent.

It is possible that rollover mitigation systems may cause the vehicle to understeer, which could lead to the activation of the ESC system to request understeer control during an RCF activation, i.e., the RCF function is counteracted by the ESC understeer control. For this reason, it is important to integrate the RCF and ESC functions.

On the other hand, if during an RCF activation ESC oversteer control is also activated, the arbitrated brake pressure should pick the maximum between the ESC oversteer control pressure command and the RCF control pressure command together with a slip control function.

Notice that RCF also must be integrated with the ABS function. While ABS aims to maintain a certain slip target to optimize stopping distance and steerability when in an ABS event, a roll mitigation system such as RCF will likely request an alternate slip target, so as to modulate lateral forces and subsequently reduce the resulting roll moment.

The RCF is targeted to reside in the brake ECU where the ABS, TCS and ESC functions reside, such that the integration between RCF and the existing functions can be easily implemented. A block diagram for such a configuration is shown in Fig. 11, where the lower block depicts the brake ECU which is divided into two parts: the lower portion contains the existing functions and their priority and arbitration logic together with all the fail-safe and interface logic; the upper portion includes the RCF and its priority logic.

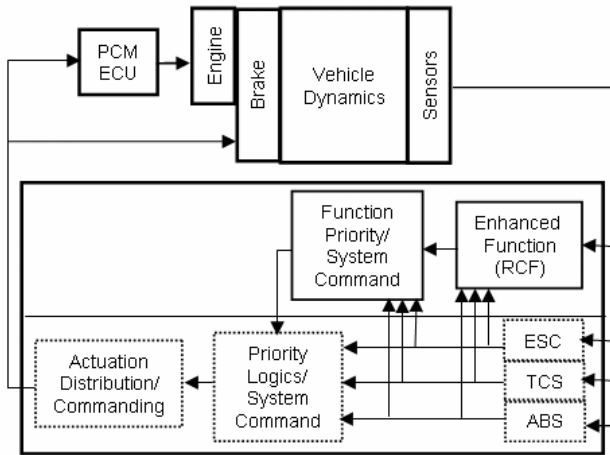


Fig. 11. Function partition in a brake control ECU

## 6. CONCLUSION

Rollover mitigation can be enhanced beyond the benefits provided by a traditional ESC system. However, when implemented with the standard ESC sensor set, this study has shown that the benefits are subject to a trade-off between the effectiveness in rollover control and the responsiveness of the vehicle in roll-stable situations.

This compromise is driven by state estimation techniques that can not differentiate among various road conditions (such as road bank) or the extremes of vehicle loading.

Continuous improvement of the system performance will likely require additional hardware. A system with additional sensors, such as the roll-rate based RSC™ system, provides the next level of system performance, where the control effectiveness and vehicle responsiveness can be simultaneously achieved. With the addition of roll-rate, the roll dynamics model can be robust to varying road conditions or varying vehicle loading. Additionally, some incremental benefit could be obtained by tailoring the level of control with information obtained from the roll-rate sensor. For example, while the yaw rate or front sideslip angle are not sensitive to roof loading or road bank, the same yaw rate or front sideslip angle could lead to a more unstable situation in a vehicle with roof load compared to a vehicle without roof load. Therefore, there could be advantages to making the controller gains and deadbands dependent on information from the roll-rate sensor.

## REFERENCES

1. A. T. van Zanten, "Bosch ESP Systems: 5 years of Experience", *SAE 2000-01-1633*.
2. A. Ungoren and H. Peng, "Rollover propensity evaluation of an SUV equipped with a TRW VSC system", *SAE 2001-01-0128*.
3. A. Hac, "Influence of active chassis systems on vehicle propensity to maneuver-induced rollovers", *SAE 2002-01-0967*.
4. L. Palkovics, A. Semsey and E. Gerum, "Rollover prevention system for commercial vehicles – additional sensorless function of the electronic brake system", *Vehicle System Dynamics*, Vol. 32, pp. 285-297, 1999.
5. T. J. Wielenga, "A method for reducing on-road rollovers – anti-rollover braking", *SAE 1999-01-0123*.
6. E. K. Liebermann, K. Meder, J. Schuh and G. Nenninger, "Safety and Performance Enhancement: the Bosch Electronic Stability Control (ESP)", *SAE 2004-21-0060*.
7. J. Lu, T. Brown and J. Meyers, "Enhanced system for yaw stability control system to include roll stability control function", *US Patent 6654674*.
8. T. Brown and D. Rhode, "Roll over stability control for an automotive vehicle", *US Patent 6263261*.
9. A. Hac, T. Brown and J. Martens, "Detection of vehicle rollover", *SAE 2004-01-1757*.
10. J. Ackermann and D. Odenthal, "Robust steering control for active rollover avoidance of vehicles with elevated center of gravity", *Proc. International Conference on Advances in Vehicle Control and Safety*, Amiens, France, July 1998.
11. Y. Lee, "Control methodology to alter automobile rollover tendencies", *NASA Tech Brief*, vol. 24, No. 4, 2000.

12. T. Shim and D. Toomey, "Investigation of active steering/wheel torque control at rollover limit maneuver", *SAE* 2004-01-2097.
13. S. Yoon, J. Jung, B. Koo and D. Kim, "Development of rollover prevention system using unified chassis control of ESP and CDC systems", *SAE* 2006-01-1276.
14. J. Lu and T. Brown, "Attitude sensing system of an automotive vehicle relative to the road", *US Patent* 6556908.
15. J. Lu, J. Meyers, M. Brewer and T. Brown, "System for dynamically determining the wheel grounding and wheel lifting conditions and their applications in roll stability control", *US Patent* 6904350.

Email: [jlu10@ford.com](mailto:jlu10@ford.com)

Dave Messih  
Supervisor  
NAE Brake Controls  
Ford Motor Company  
2400 Village Rd, P.O. Box 2053  
Dearborn, MI 48124  
Email: [dmessih@ford.com](mailto:dmessih@ford.com)

Albert Salib  
Senior Engineer  
NAE Brake Controls  
Ford Motor Company  
2400 Village Rd, P.O. Box 2053  
Dearborn, MI 48124  
Email: [asalib@ford.com](mailto:asalib@ford.com)

## CONTACTS

Jianbo Lu, Ph.D.  
Technical Expert  
Active Safety Research & Advanced Engineering  
Ford Motor Company  
20300 Rotunda Dr.  
Dearborn, MI 48124

Dave Harmison  
Development Engineer  
NAE Brake Controls  
Ford Motor Company  
2400 Village Rd, P.O. Box 2053  
Dearborn, MI 48124  
Email: [dharmiso@ford.com](mailto:dharmiso@ford.com)